Annals of Nuclear Energy 90 (2016) 54–61

Contents lists available at ScienceDirect

Annals of Nuclear Energy

journal homepage: www.elsevier.com/locate/anucene

Temperature control characteristics analysis of lead-cooled fast reactor with natural circulation

Minghan Yang, Yong Song *, Jianye Wang, Peng Xu, Guangyu Zhang

Key Laboratory of Neutronics and Radiation Safety, Institute of Nuclear Energy Safety Technology, Chinese Academy of Sciences, Hefei, Anhui 230031, China

ARTICLE INFO

Article history:
Received 9 July 2015
Received in revised form 18 November 2015
Accepted 19 November 2015
Available online 18 December 2015

Keywords:
LFR
Natural circulation
Temperature control characteristic
Transfer function matrix
Frequency domain analysis method

ABSTRACT

Lead-cooled Fast Reactor (LFR) with natural circulation in primary system is among the highlights in advance nuclear reactor research, due to its great superiority in reactor safety and reliability. In this work, a transfer function matrix describing coolant temperature dynamic process, obtained by Laplace transform of the one-dimensional system dynamic model is developed in order to investigate the temperature control characteristics of LFR. Based on the transfer function matrix, a close-loop coolant temperature control system without compensator is built. The frequency domain analysis indicates that the stability and steady-state of the temperature control system needs to be improved. Accordingly, a temperature compensator based on Proportion–Integration and feed-forward is designed. The dynamic simulation of the whole system with the temperature compensator for core power step change is performed with SIMULINK and RELAP5-HD. The result shows that the temperature compensator can provide superior coolant temperature control capabilities in LFR with natural circulation due to the efficiency of the frequency domain analysis method.

1. Introduction

The lead cooled fast reactor (LFR) is envisaged as one of the six promising nuclear energy technologies for future advanced systems and is also considered as the system to burn actinides currently (Bianchi et al., 2006). Compared to other kinds of nuclear reactors, LFR has many inherent advantages (Wu et al., 2016):

(a) High boiling temperature and low melting temperature.
(b) Large heat capacity.
(c) No energetic reaction with air and water.
(d) Better shielding against gamma rays and energetic neutrons.

Because of the above advantages, LFR has become the research focus during recent years, several LFRs had been designed in many countries: SVBR (Zrodnikov et al., 2008) and BREST (Orlov et al., 2005) in Russia, MYRRHA (De Bruyn et al., 2007) and ElSY (Cinotti et al., 2008) in Europe, SSTR (Smith et al., 2008) in U.S. In China, series innovative lead-based reactors concepts and some key technology had been developed by FDS Team, such as subcritical system (Wu et al., 2011; Wu and FDS Team, 2008) neutron transport calculation (Wu et al., 1999, 2002; Wu, 2007), liquid metal coolant technology (Wu and FDS Team, 2011), structure materials (Wu and FDS Team, 2009; Huang et al., 2011, 2004), reactor design, etc. However, according to the related published articles, LFRs have rarely been in operation all over the world, except Russia where LFRs were applied in submarines during mid 1960s to 1990s (Alemberti et al., 2014).

In order to study temperature control characteristics, a transfer function model of LFR coolant system is necessary. Since the accurate three-dimensional dynamic model is too complex to be used in derivation of transfer function model, one-dimensional distributed parameter model is employed to be linearized in time domain, and discretized in Spatial Domain for transfer function modeling. A transfer function matrix describing coolant temperature dynamic process is obtained by Laplace transform of the one-dimensional model. This transfer function matrix provides the possibility that the characteristics of the coolant temperature control system can be analyzed by classical frequency domain analysis method of Single-Input–Single-Output System. The frequency domain analysis indicates that the coolant temperature control system without compensator is instable and the steady state error cannot be eliminated completely. Therefore, a temperature compensator based on Proportion–Integration and feed-forward is designed for improving the system performance. Proportion term improves the stability, integration eliminates steady state error, and feed-forward improves the response rate. The sim-

* Corresponding author.
E-mail address: yong.song@fds.org.cn (Y. Song).

http://dx.doi.org/10.1016/j.anucene.2015.11.029
0306-4549/

Nomenclature

c	thermal capacity
d	diameter
D	PID controller
e	steady state error
F	area of heat transfer per unit length
f	mass force
FW	ideal feed forward controller
FW'	feed forward controller designed for this work
G	mass flow rate
h	enthalpy
K	open loop gain
Ki	integral coefficient of the compensation
Kp	proportionality coefficient of the compensation
l	the length of the node
m	mass per unit length
M	closed loop transfer function
N^+	the number of clockwise encirclements of point $(-1, j0)$ by Nyquist curves
P	the number of poles of $W_{airgin-hextout}$ and $W_{hexgin-hextout}$ in closed right-half plane
q	thermal power
s	Laplace operator
t	time
Tf	transfer function matrix
Th	the matrix contains input or output variables
W	open loop transfer function
z	coordinates in space
α	coefficient of heat transfer
β	proportionality coefficient between $\Delta\rho$ and Δh
γ	proportionality coefficient between ΔT and $\Delta\rho$
Δ	property variation (perturbation around steady-state condition)
η	proportionality coefficient between ΔT and ΔH
ρ	density
τ	time delay of system

Subscripts

airgin	inlet air mass flow rate of air cooler
clad	clad surrounding the fuel node
corein	core inlet temperature
coreout	core outlet temperature
fuel	fuel
gap	gap between fuel and clad
GG	from inlet mass flow rate to outlet mass flow rate in one node
Gh	from inlet mass flow rate to outlet enthalpy in one node
hextout	outlet temperature on secondary side of heat exchanger
hG	from inlet enthalpy to outlet mass flow rate in one node
hh	from inlet enthalpy to outlet enthalpy in one node
in	inlet of the node
*in*0	initial value of inlet parameter in one node
j	*j*th node
l	coolant node with length *l*
out	outlet of the node
*out*0	initial value of outlet parameter in one node
p	primary side
pumpgout	outlet mass flow of pump in secondary
s	secondary side
w	wall of the pipe

ulation result presents that the temperature compensator could provide superior coolant temperature control capabilities in LFR with natural circulation.

2. Coolant system transfer function model

2.1. Main design parameters of the reactor

The 10 MWth LBE-cooled pool type fast reactor driven by the natural circulation is designed. UO_2 is selected as the fuel whose U^{235} mass enrichment is about 19.75%.The LBE is selected as the coolant for the primary loop. The average inlet and outlet LBE temperatures of the core are about 535 K and 665 K, respectively. The cover gas pressure in the primary loop is about 0.05 MPa. Pressurized water (4 MPa) is chosen as the secondary circuit coolant. The average inlet and outlet water temperature of the heat exchanger (HEX) are about 490 K and 501 K, respectively. The heat generated in the reactor is released to the final sink (atmosphere) by an air cooler. The main parameters of the natural circulation LBE-cooled fast reactor core are shown in Table 1.

2.2. Transfer function modeling

In this section, the discussion is aimed at the transfer function modeling method of the coolant temperature dynamic process in the reactor. For simplification, a single phase heat exchange tube model is referenced. The other models, such as reactor core model, primary and secondary heat-exchanger (HEX) model, are formally equivalent.

The first principle method of thermal-hydraulic has been considered to describe the thermal-hydraulic dynamic behavior of the reactor:

$$\frac{\partial\rho}{\partial t}+\frac{\partial G}{\partial z}=0 \tag{1}$$

$$\frac{\partial(\rho h)}{\partial t}+\frac{\partial(Gh)}{\partial z}-q_l=0 \tag{2}$$

According to the method of Colombo et al. (2010), shown as Fig. 1 (the length of each node is l, and the number of the nodes is n), the transfer function matrix can be deduced according to backward finite difference scheme:

$$\begin{pmatrix}\Delta h_{out}(s)\\ \Delta G_{out}(s)\end{pmatrix}=Tf\begin{pmatrix}\Delta h_{in}(s)\\ \Delta G_{in}(s)\\ \Delta q_l(s)\end{pmatrix} \tag{3}$$

where

$$Tf(s)=\begin{pmatrix}\frac{G_{out0}}{l\rho_{out0}s+G_{out0}} & \frac{h_{in0}-h_{out0}}{l\rho_{out0}s+G_{out0}} & \frac{1}{l\rho_{out0}s+G_{out0}}\\ \frac{-\beta lG_{out0}s}{l\rho_{out0}s+G_{out0}} & \frac{[\rho_{out0}-\beta(h_{in0}-h_{out0})]ls+G_{out0}}{l\rho_{out0}s+G_{out0}} & \frac{-\beta ls}{l\rho_{out0}s+G_{out0}}\end{pmatrix} \tag{4}$$

In this model, the dependence of fluid density on enthalpy can be accounted:

$$\Delta\rho=\beta\Delta h \tag{5}$$

Table 1
Main geometrical parameters of the natural circulation LBE-cooled fast reactor core.

Parameter	Unit	Value
Core power	MW	10
Core inlet temperature	K	535
Core outlet temperature	K	665
Fission fuel	–	UO_2(19.75%)
Driving force on the LBE	–	Buoyancy force
Secondary coolant	–	Water
Secondary loop coolant pressure	MPa	4
HEX secondary side coolant inlet temperature	K	490
HEX secondary side coolant outlet temperature	K	501
Heat sink	–	Air cooler
Cladding	–	316Ti
Structure	–	316L

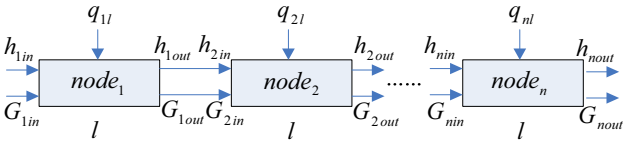

Fig. 1. The structure of the single phase tube model.

Eqs. (3) and (4) is the linear time-invariant thermal hydraulic transfer function model which links the three system inputs to the two system outputs. Single phase tube has n nodes can be described as follow equations:

$$Th_{jout}(s) = Tf_j(s) \times Th_{jin}(s) \tag{6}$$

$$Th_{(j+1)in}(s) = \begin{pmatrix} Th_{jout}(s) \\ \Delta q_{(j+1)l}(s) \end{pmatrix} \tag{7}$$

where Tf_j means the transfer function matrix of j th node in the tube, $1 \le j \le n$. Th_{jin} and Th_{jout} are described as follows:

$$Th_{jin} = \begin{pmatrix} \Delta h_{jn}(s) \\ \Delta G_{jn}(s) \\ \Delta q_{jl}(s) \end{pmatrix} \tag{8}$$

$$Th_{jout} = \begin{pmatrix} \Delta h_{jout}(s) \\ \Delta G_{jout}(s) \end{pmatrix} \tag{9}$$

(1) The core transfer function modeling

A one-dimensional single channel core thermal model can be shown as Fig. 2 (Heat transfer process in radial direction is neglected. In Z direction, fuel, gap, clad and coolant are divided into n nodes with length l). In this model, the coordinate of fuel rod central axis is zero.

According to the Heat Diffusion Equation, the transfer function of heat transfer process from fuel to clad can be represented as follows:

$$\Delta T_{cladj}(s) = \frac{\alpha_{gap} f_{gap} \Delta T_{gapj}(s) + \alpha_{clad} f_{clad} \Delta T_{jin}(s)}{m_{cladj} c_{cladj} s + \alpha_{gap} f_{gap} + \alpha_{clad} f_{clad}} \tag{10}$$

$$\Delta T_{gapj}(s) = \frac{\alpha_{fuel} f_{fuel} \Delta T_{fuelj}(s) + \alpha_{gap} f_{gap} \Delta T_{cladj}(s)}{m_{gapj} c_{gapj} s + \alpha_{fuel} f_{fuel} + \alpha_{gap} f_{gap}} \tag{11}$$

$$\Delta T_{fuelj}(s) = \frac{\Delta q_{fuelj} + \alpha_{fuel} f_{fuel} \Delta T_{gapj}(s)}{m_{fuelj} c_{fuelj} s + \alpha_{fuel} f_{fuel}} \tag{12}$$

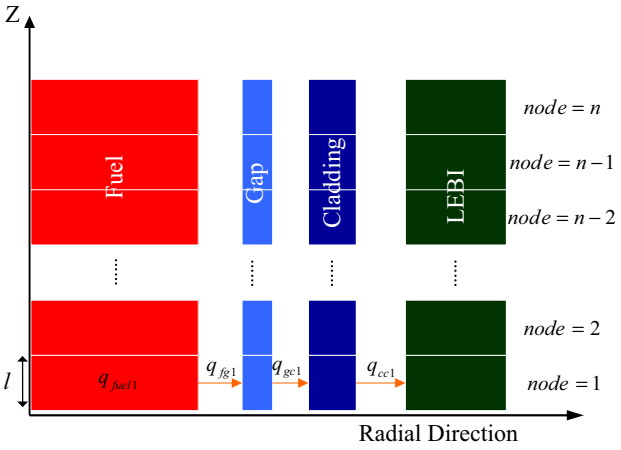

Fig. 2. The one-dimension heat transfer model of reactor core.

$$\Delta q_{lj}(s) = \frac{\alpha_{clad} f_{clad} (\Delta T_{cladj}(s) - \Delta T_{jin}(s))}{4l/d} \tag{13}$$

According to the Boussinesq Approximation, the dependence of temperature on density can be accounted in natural circulation (Sabharwall et al., 2012):

$$\Delta T = \gamma \Delta \rho \tag{14}$$

where γ is constant coefficient.

Consider the Eq. (5), one has:

$$\Delta T = \eta \Delta H \tag{15}$$

where

$$\eta = \gamma \cdot \beta \tag{16}$$

Thermal power variable Δq_{fuelj} can be regarded as input of core heat transfer system. For another, temperature variables ΔT_{fuelj} ΔT_{gapj} ΔT_{cladj} can be calculated by Eqs. (10)–(12). Eqs. (3) and (10)–(13) constitute the transfer function model of heat transfer process in reactor core.

(2) The HEX transfer function modeling

The HEX is simplified to straight tubes, single pass model (Fig. 3) where LBE flow down on the primary side and single phase water flow up on the secondary side. Therefore, the transfer functions of heat transfer process between LBE, wall and water can be described as:

$$\Delta T_{wj}(s) = \frac{\alpha_{ws} f_{ws} \Delta T_{sjin}(s) + \alpha_{wp} f_{wp} \Delta T_{pjin}(s)}{m_{wj} c_{wj} s - \alpha_{wp} f_{wp} + \alpha_{ws} f_{ws}} \tag{17}$$

$$\Delta q_{plj}(s) = \frac{\alpha_{wp} f_{wp} (\Delta T_{wj}(s) - \Delta T_{pjin}(s))}{4l_p/d_p} \tag{18}$$

$$\Delta q_{slj}(s) = \frac{\alpha_{ws} f_{ws} (\Delta T_{wj}(s) - \Delta T_{sjin}(s))}{4l_s/d_s} \tag{19}$$

Eqs. (3) and (17)–(19) constitute the transfer function model of heat transfer process in HEX, which can be shown as Fig. 3 (heat transfer between adjacent nodes of tube wall is neglected).

(3) The coolant channel transfer function modeling

It is assumed that the coolant channel, consist of upper channel, upper plenum, down comer and down plenum, is thermally isolated, and heat transfer between adjacent tube wall nodes is

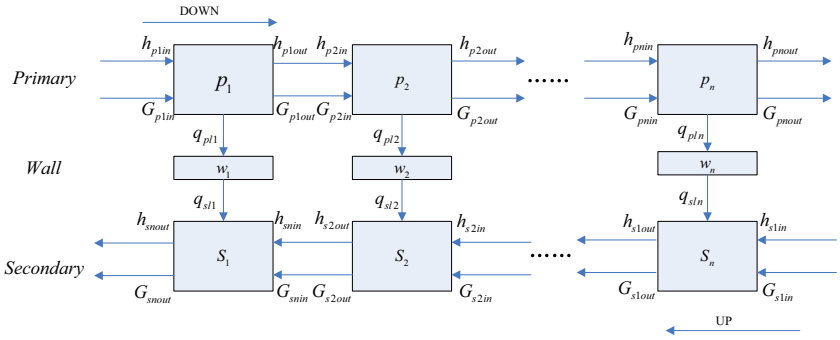

Fig. 3. Structure of the heat-exchanger model has n nodes, include primary side, secondary side and tube wall.

neglected. According to the method in Section 3.1, the j th coolant channel node transfer function modeling can be given with inserting $\Delta q_l = 0$:

$$\begin{pmatrix} \Delta h_{jout}(s) \\ \Delta G_{jout}(s) \end{pmatrix} = \begin{pmatrix} TF_{hh} & TF_{Gh} \\ TF_{hG} & TF_{GG} \end{pmatrix} \begin{pmatrix} \Delta h_{jin}(s) \\ \Delta G_{jin}(s) \end{pmatrix} \tag{20}$$

where

$$TF_{hh} = \frac{G_{jout0}}{l\rho_{jout0}s + G_{jout0}} \tag{21}$$

$$TF_{Gh} = \frac{h_{jin0} - h_{jout0}}{l\rho_{jout0}s + G_{jout0}} \tag{22}$$

$$TF_{hG} = \frac{-\beta l G_{out0}s}{l\rho_{jout0}s + G_{jout0}} \tag{23}$$

$$TF_{GG} = \frac{[\rho_{out0} - \beta(h_{in0} - h_{out0})]ls + G_{out0}}{l\rho_{jout0}s + G_{jout0}} \tag{24}$$

(4) Air cooler and pump

It can be considered that the air-cooler has the same structure as the HEX. The flow rate boundary is used instead of the pump in the secondary loop and the fan in the air-cooler.

3. Frequency domain analysis and compensator design

In this section, a temperature control strategy is presented first. Based on this strategy, a temperature control loop without any compensator is built, and analyzed in frequency domain. The analysis gives the characteristics of temperature control system, including stability and steady-state. According to the analysis result, a temperature controller for system compensation is designed. Moreover, a feed-forward controller is also introduced to compensate the large time-lag in temperature control system.

3.1. Temperature control strategy

The aim of temperature control system is to ensure the safety of coolant system under power perturbation. For a reactor, the critical variables are the coolant temperature in core and HEX, which can reflect the energy flow state and security feature in the reactor. Accordingly, there are two control strategies: (1) keeping coolant temperature constant in the core (control strategy A) (Yan et al., 2014); (2) keeping the coolant outlet temperature constant in HEX secondary side (control strategy B). The main advantage of control strategy A is to ensure the security of primary loop and avoid the core meltdown or LBE solidification. However, control strategy A may cause large changes in the pressure and temperature of secondary loop. In the reference design of Section 2.1, the coolant in secondary loop is single-phase water with 4 MPa. The large pressure and temperature change may lead to serious problems in single-phase water loop. Therefore, control strategy B is adopted in this work. Due to the enough security margin of LBE, the temperature in core is also safely under power disturbance.

Fig. 4 shows the control loop without any compensator. Where $T_{hexwout}$ is the controlled variable, which could be regulated by the air-cooler and pump. The core power perturbation Δq is system disturbance. The reference value of $T_{hextout}$ is 501 K.

3.2. Selection of analysis method

Root locus, magnitude-phase characteristics curves (Nyquist) and logarithmic frequency characteristic curves (Bode) are system analysis tools which have their own characteristic. An appropriate system analysis tool needs to be selected from the above three analysis tools. The distributions of open-loop zeros and poles can provide a reference for the analysis tool selection.

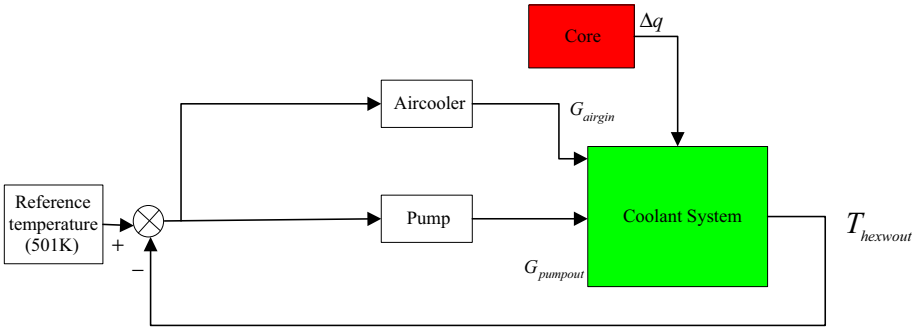

Fig. 4. The control loop without any compensators.

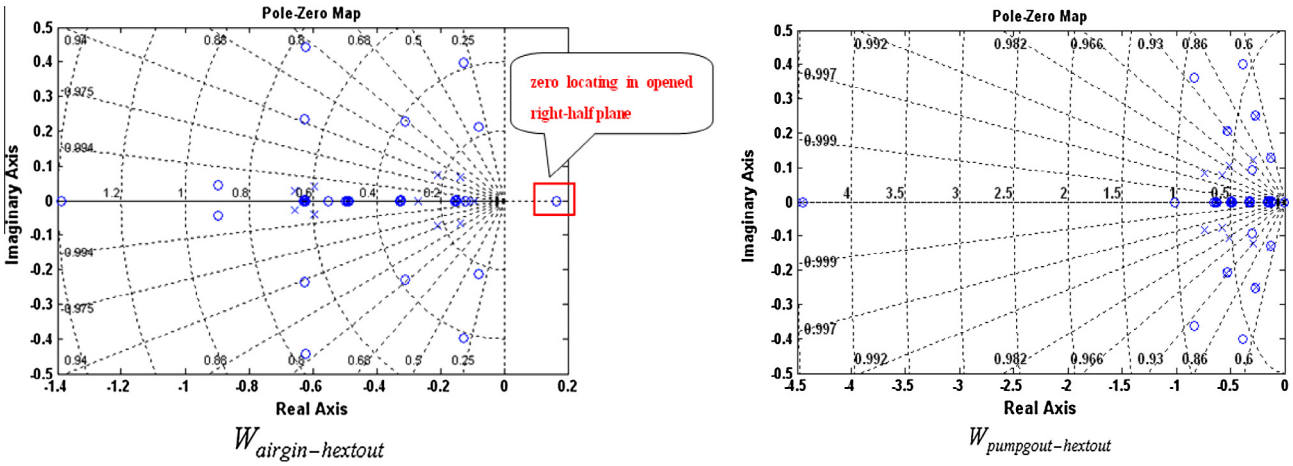

Fig. 5. Zeros and poles distributions of $W_{airgin-hextout}$ and $W_{pumpgout-hextout}$, where 'X' means pole, 'o' means zero.

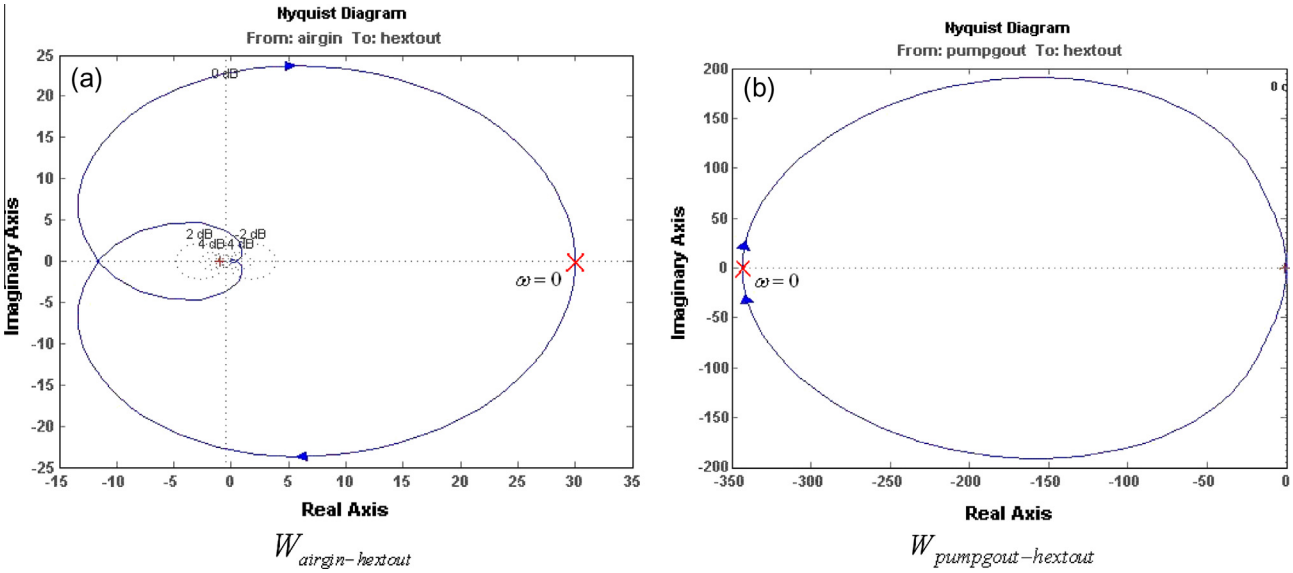

Fig. 6. Nyquist curves of $W_{airgin-hextout}$ and $W_{pumpgout-hextout}$.

According to the Fig. 4, open-loop transfer functions of the system are $W_{airgin-hextout}$ and $W_{pumpgout-hextout}$. The transfer function matrix in Section 2 indicates the coolant system has a complex multi-channel structure. Therefore, zeros and poles of $W_{airgin-hextout}$ and $W_{pumpgout-hextout}$ are difficult to be solved directly. For this reason, the linear system analysis tool of SIMULINK (2007) is adopted to calculate the distributions. The poles and zeros distributions of $W_{airgin-hextout}$ and $W_{pumpgout-hextout}$ given by the linear system analysis tool of Simulink are shown as Fig. 5.

Two important characteristics of these transfer functions can be concluded from Fig. 5: (1) there is a large number of zeros and poles in the pole–zero maps, and dominant poles are difficult to be extracted; (2) there is a zero of $W_{airgin-hextout}$ locate in opened right-half plane. The first point means root locus method cannot be used for analysis of $W_{airgin-hextout}$ and $W_{pumpgout-hextout}$ because the root locus plots are extremely complex and cannot be simplified according to the dominant poles; the secondary point means Bode curves is also not available because it cannot be used for stability analysis of non-minimum system (Benjamin, 2003). Therefore, only the Nyquist curves can be selected as an analysis tool for $W_{airgin-hextout}$ and $W_{pumpgout-hextout}$.

3.3. Frequency domain analysis with Nyquist

(1) Steady state

According to the Nyquist curves of $W_{airgin-hextout}$ and $W_{pumpgout-hextout}$ (Fig. 6), the steady state gains of these two transfer functions ($\omega = 0$) is limited (steady state gains of $W_{airgin-hextout}$ is about 30 dB, steady state gains of $W_{airgin-hextout}$ is about 345 dB). It means steady state error of close-loop $M_{airgin-hextout}$ and $M_{pumpgout-hextout}$ under the step input cannot be eliminated completely.

(2) Stability

According to the Nyquist criterion, $M_{airgin-hextout}$ and $M_{pumpgout-hextout}$ without any compensator are instability because $N^+ + P \neq 0$, where, N^+ is the number of clockwise encirclements of point $(-1, j0)$ by Nyquist curve, P is the number of poles of $W_{airgin-hextout}$ and $W_{hexgin-hextout}$ in closed right-half plane.

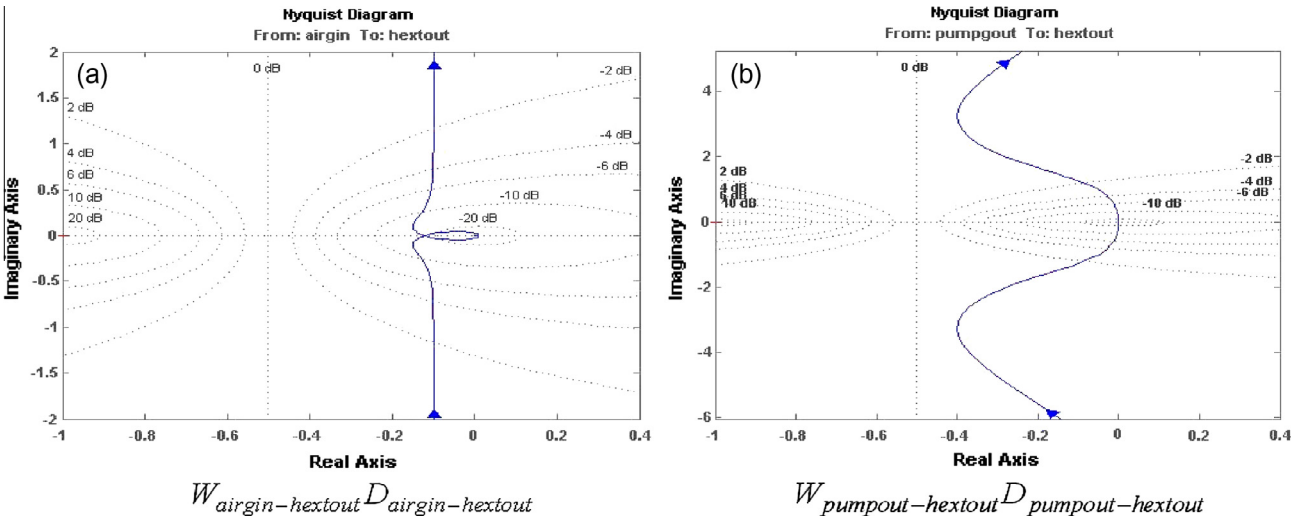

Fig. 7. Nyquist curves of $W_{airgin-hextout}D_{airgin-hextout}$ and $W_{pumpgout-hextout}D_{pumpgout-hextout}$.

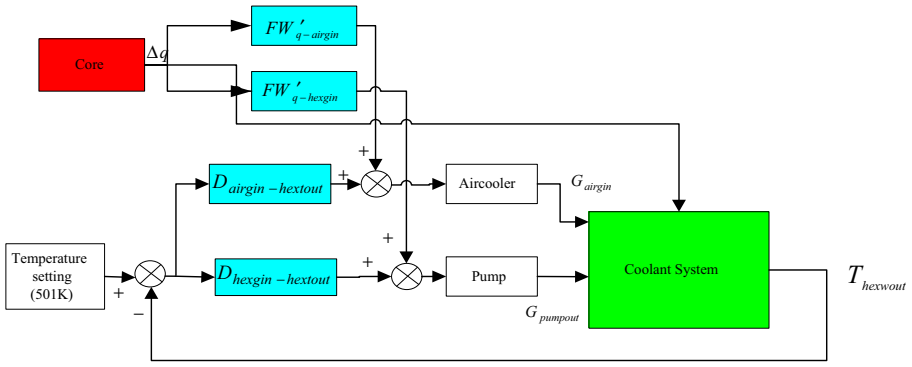

Fig. 8. Temperature control system with PI and feed-forward compensator.

3.4. Proportion–Integration compensator design

The frequency domain analysis shows that a compensator needs to be designed for the improving stability and eliminating the steady state error of control system in Fig. 4. For this purpose, Proportional-Integral (PI) controller is introduced as system compensator (Yoshiaki et al., 2013). The controller expressions can be shown as follows:

$$D_{airgin-hextout} = Kp_{airgin-hextout} + \frac{Ki_{airgin-hextout}}{s} \tag{25}$$

$$D_{pumpgout-hextout} = Kp_{pumpgout-hextout} + \frac{Ki_{pumpgout-hextout}}{s} \tag{26}$$

The Nyquist curves of $W_{airgin-hextout}D_{airgin-hextout}$ and $W_{pumpgout-hextout}D_{pumpgout-hextout}$ are shown as Fig. 7. It can be found that the control loop with compensators $D_{airgin-hextout}$ and $D_{pumpgout-hextout}$ is stability because of $N^+ = 0$ and $P = 0$. $Kp_{airgin-hextout}$ and $Kp_{pumpgout-hextout}$ can bring great stability margin which can make system steady running when system devices parameters drift. When $\omega = 0$, steady state gains of $W_{airgin-hextout}D_{airgin-hextout}$ and $W_{pumpgout-hextout}D_{pumpgout-hextout}$ are infinity because the Integral elements improve the steady state characteristic. Eqs. (27) and (28) show steady state error of the control loop under step input:

$$\begin{aligned} e_{airgin-hextout} &= \lim_{s\to 0} s \cdot \frac{1}{1 + D_{airgin-hextout}W_{airgin-hextout}} \cdot \frac{1}{s} \\ &= \lim_{s\to 0} \frac{s}{s + (Kp_{airgin-hextout}s + Ki_{airgin-hextout})W_{airgin-hextout}} \\ &= 0 \end{aligned} \tag{27}$$

$$\begin{aligned} e_{pumpgout-hextout} &= \lim_{s\to 0} s \cdot \frac{1}{1 + D_{pumpgout-hextout}W_{pumpgout-hextout}} \cdot \frac{1}{s} \\ &= \lim_{s\to 0} \frac{s}{s + (Kp_{pumpgout-hextout}s + Ki_{pumpgout-hextout})W_{pumpgout-hextout}} \\ &= 0 \end{aligned} \tag{28}$$

3.5. Feed-forward compensator design

Consider the time constant in transfer function matrix (Eq. (4)):

$$\tau = \frac{l\rho_{jout0}}{G_{jout0}} = \frac{l}{v_{jout0}} \tag{29}$$

Eq. (29) shows the large delay time in components of coolant system, thus a feed forward scheme has been adopted for improving the dynamic response of the control system:

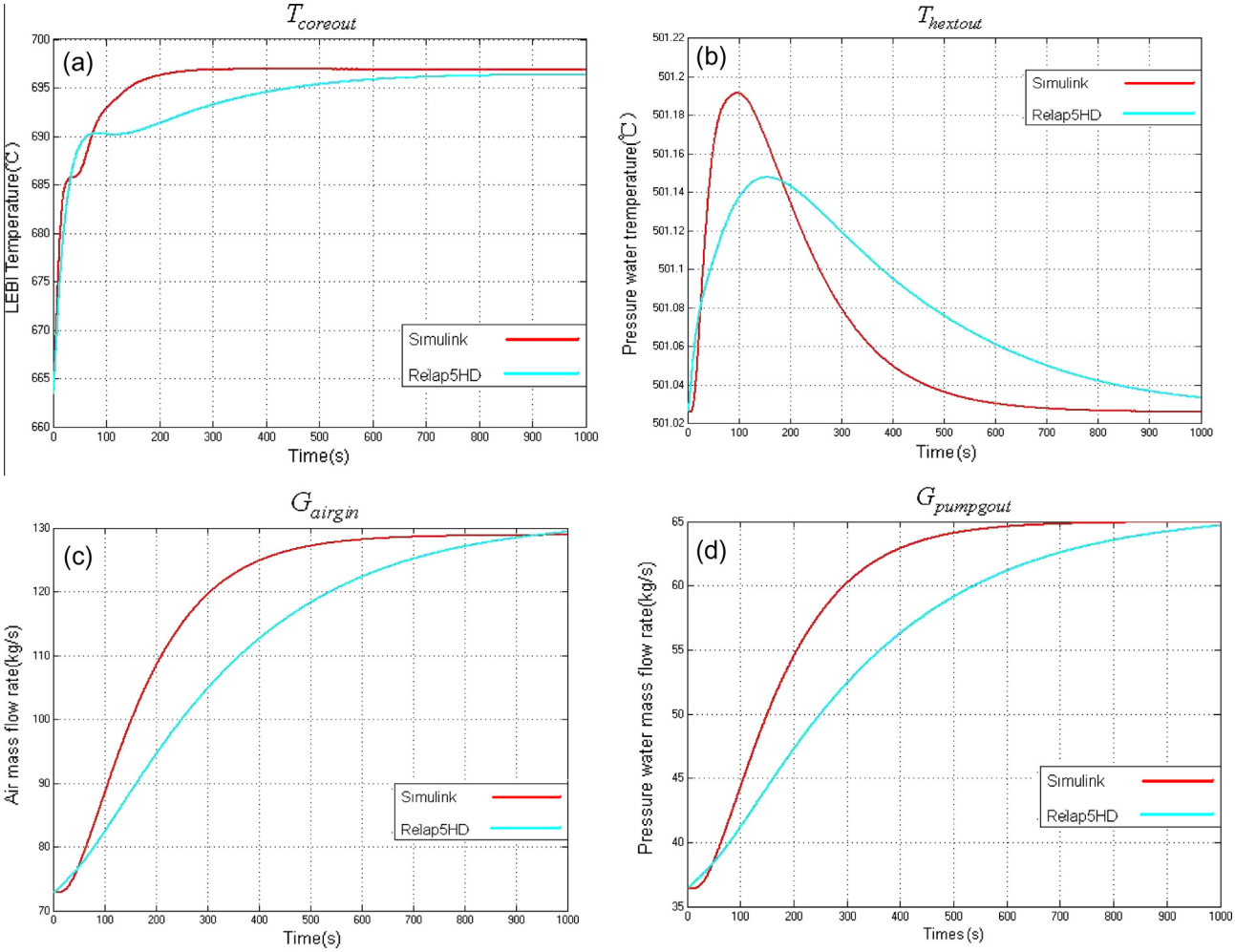

Fig. 9. System response to reactor power change (30% of RFP) with PI and feed-forward compensator.

$$FW_{q-airgin} = \frac{W_{q-hextout}}{W_{airgin-hextout}} \tag{30}$$

$$FW_{q-pumpgout} = \frac{W_{q-hextout}}{W_{pumpgout-hextout}} \tag{31}$$

Theoretically, $FW_{q-airgin}$ and $FW_{q-pumpgout}$ given by Eqs. (30), (31) can eliminate the temperature error accurately; however, it is hard to realize actually because of high order in $W_{q-hextout}$, $W_{airgin-hextout}$, $W_{q-hextout}$ and $W_{pumpgout-hextout}$. A lead–lag component can be introduced to instead of $FW'_{q-airgin}$ and $FW'_{q-pumpgout}$:

$$FW'_{q-airgin} = K_{f1}\frac{1+T_1 s}{1+T_2 s} \tag{32}$$

$$FW'_{q-pumpgout} = K_{f2}\frac{1+T_3 s}{1+T_4 s} \tag{33}$$

where $T_2 = \tau_{q-hextout} - \tau_{airgin-hextout}$, $T_4 = \tau_{q-hextout} - \tau_{pumpgout-hextout}$. K_{f1} and K_{f2} can be set to the steady-state of air mass flow rate and outlet temperature in secondary side of HEX. T_1 and T_3 can be adopted to improve the dynamic characteristic of the feed forward controller.

The block diagram of temperature control system with PI and feed-forward compensator can be shown as Fig. 8.

4. Simulation result

To verify the efficiency of the control strategy and the capabilities of the temperature compensator, the core power step change is simulated by Simulink. The reactor initially operates at 100% Rated Full Power (RFP). The power steps to 130% RFP at 1st second. The response of $T_{coreout}$, $T_{hextout}$, G_{airgin} and $G_{pumpout}$ can be shown as Fig. 9 ([1]red lines). As comparison, the reactor dynamic model with Relap5-HD (2011) has also been simulated in Fig. 9 (Brilliant blue lines). It can be found that T_{hexout} keeps constant under the action of $D_{airgin-hexout}$ and $D_{hexgin-hexout}$ (maximum temperature fluctuation is less than 0.2 K), accordingly the pressurizer of secondary loop needs not to bear the large pressure change. In the primary loop, the coolant temperature is in safe level and has large security margin.

5. Summary

In this work, a transfer function model on the basis of the fundamental conservation laws of mass and energy which describes the temperature dynamic process of primary and secondary loop in the LFR is built. Based on the transfer function model, a coolant temperature control system to keep outlet temperature constant in

[1] For interpretation of color in Fig. 9, the reader is referred to the web version of this article.

secondary side of HEX is analyzed through frequency domain analysis method. The frequency analysis shows the temperature control system without compensator of the LFR with natural circulation is instable and has limited steady state gains. Accordingly, a temperature compensator based on PI and feed-forward is designed for improving the system performance. To show efficiency and feasibility of the temperature compensator, the dynamic simulation of the whole system with temperature compensator in the case of core power step change (30% of RFP) is performed. The simulation result shows the outlet temperature in secondary side of HEX is well controlled and other key parameters are in allowable range. Thus, the compensator designed by frequency domain method has superior coolant temperature control capabilities in LFR with natural circulation. It also presents that the frequency domain method is a useful tool for study of LFR operation and control.

In the future work, the accuracy of the transfer function model based on the first principle method will be verified through the LBE thermal-hydraulic experimental loop.

Acknowledgement

This work was supported by 'Strategic Priority Research Program' of the Chinese Academy of Sciences Grant No. XDA03040000. We further thank the other members of FDS Team for the great help in this research.

References

Alemberti, A., Smirnov, V., Smith, C.F., et al., 2014. Overview of lead-cooled fast reactor activities. Prog. Nucl. Energy 77, 300–307.

Benjamin, C., 2003. Automatic Control Systems. John Wiley & Sons Inc., Hoboken.

Bianchi, F., Artioli, C., Burn, K.W., et al., 2006. Status and trend of core design activities for heavy metal cooled accelerator driven system. Energy Convers. Manage. 47, 2698–2709.

Cinotti, L., Locatelli, G., AitAbderrahim, H., Monti, S., Benamati, G., Tucek, K., Struwe, D., Orden, A., Corsini, G., Le Carpentier, D., 2008. The ELSY project. In: Proceedings of International Conference on the Physics of Reactors, PHYSOR'08 'Nuclear Power: A Sustainable Resource', Interlaken, Switzerland, 14–19 September 2008.

Colombo, M., Cammi, A., Memoli, V., et al., 2010. Transfer function modeling of the Lead-cooled Fast Reactor (LFR) dynamics. Prog. Nucl. Energy 52, 715–729.

De Bruyn, D., Maes, D., Mansani, L., Giraud, B., 2007. From MYRRHA to XT-ADS: the design evolution of an experimental ADS system. In: AccApp'07, Pocatello, Idaho, July 29–August 2, 2007.

Huang, Q., Li, J., Chen, Y., 2004. Study of irradiation effects in China low activation martensitic steel CLAM. J. Nucl. Mater. 329, 268–272.

Huang, Q., Li, C., Wu, Q., Liu, S., Gao, S., Gao, Z., et al., 2011. Progress in development of CLAM steel and fabrication of small TBM in China. J. Nucl. Mater. 417, 85–88.

Orlov, V.V., Filin, A.I., Lopatkin, A.V., Glazov, A.G., Sukhanov, L.P., Volk, V.L., Poluektov, P.P., Ustinov, O.A., Vorontsov, M.T., Leontiev, V.F., Karimov, R.S., 2005. The closed o-site fuel cycle of the BREST reactors. Prog. Nucl. Energy 47, 171–177.

Relap5-HD Software, 2011. GSE Systems Inc.

Sabharwall, P., Yoo, Y.J., Wu, Q., Sienicki, J.J., 2012. Natural circulation and linear stability analysis for liquid-metal reactors with the effect of fluid axial conduction. Nucl. Technol. 173, 301–302.

SIMULINK Software, 2007. The Math Works Inc.

Smith, C.F., Halsey, W.G., Brown, N.W., Sienicki, J.J., Moisseytsev, A., Wade, D.C., 2008. SSTAR: the US Lead-cooled Fast Reactor (LFR). J. Nucl. Mater. 376, 255–259.

Wu, Y., 2007. Progress in fusion-driven hybrid system studies in China. Fusion Eng. Des. 63–64, 73–80.

Wu, Y.FDS Team, 2008. Conceptual design of the China fusion power plant FDS-II. Fusion Eng. Des. 83, 1683–1689.

Wu, Y.FDS Team, 2009. Fusion-based hydrogen production reactor and its material selection. J. Nucl. Mater. 386–388, 122–126.

Wu, YicanFDS Team, 2011. Overview of liquid lithium lead breeder blanket program in China. Fusion Eng. Des. 86, 2343–2346.

Wu, Y., Xie, Z., Fischer, U., 1999. A discrete ordinates nodal method for one-dimensional neutron transport calculation in curvilinear geometries. Nucl. Sci. Eng. 133, 350–357.

Wu, Y., Zhu, X., Zheng, S., et al., 2002. Neutronics analysis of dual-cooled waste transmutation blanket for the FDS. Fusion Eng. Des. 63–64, 133–138.

Wu, Y., Jiang, J., Wang, M., Jin, M.FDS Team, 2011. A fusion-driven subcritical system concept based on viable technologies. Nucl. Fusion 51, 103036.

Wu, Y., Bai, Y., Song, Y., Huang, Q., Zhao, Z., Hu, L., 2016. Development strategy and conceptual design of china lead-based research reactor. Ann. Nucl. Energy 87, 511–516.

Yan, Shoujun, Fang, Huawei, Wang, Pengfei, Sun, Changyi, Zhao, Fuyu, Huang, Hao, 2014. Modeling and control strategy of the China accelerator driven subcritical reactor. Prog. Nucl. Energy 71, 179–187.

Yoshiaki, O., Haruki, M., Mitsuru, U., 2013. Nuclear Reactor Kinetics and Plant Control. Springer, Japan.

Zrodnikov, A.V., Toshinsky, G.I., Komlev, O.G., Dragunov, Y.G., Stepanov, V.S., Klimov, N.N., Generalov, V.N., Kopytov, I.I., Krushelnitsky, V.N., 2008. Innovative nuclear technology based on modular multi-purpose lead-bismuth cooled fast reactors. Prog. Nucl. Energy 50, 170–178.